

Identification of Samples From
Gentzler Area, Stevens Co., Kansas
Submitted to Reservoirs, Inc. for Analysis

Thin Section Petrography

Sample #1A	Gaskill A-2	SE Sec. 10-33S-38W
#2	"	
#5	"	
#7	"	

Scanning Electron Microscopy

Sample #1A	Gaskill A-2
#2	"

X-Ray Diffraction

Sample #1A	Gaskill A-2	6053'
#1	"	6008'
#2	"	6013'
#3	"	6015'
#4	"	6018'
#5	"	6028'
#6	"	6055'
#7	"	6066'
#8	Youngren B-2	NW Sec. 13-32S-39W 5850-60'
#9	Methodist C-1	SW Sec. 17-32S-37W 6040-60'
#10	Shell 3-13	NE Sec. 13-33S-38W 6010-60'
#11	Guyer B-1	SW Sec. 3-33S-38W 6020-60'
#12	Nell A-1	NW Sec. 19-33S-37W 6050-6110'
#13	Crawford C-1	NW Sec. 29-33S-37W 6060-6100'
#14	Stout C-1	NE Sec. 32-32S-38W 6020-40'
#15	Hickok B-1	NE Sec. 13-32S-39W 5820-70'
#16	Bane H-1	NE Sec. 1-33S-38W 6010-90'
#17	Curtis B-1	SE Sec. 6-32S-38W 5840-5890'
#18	Roberts A-1	SW Sec. 20-33S-37W 6050-6110'
#19	Kuharic A-1	SW Sec. 6-33S-37W 6000-6040'

THE LITHOLOGY, CLAY MINERALOGY, AND COMPLETION SENSITIVITY OF
SELECTED SANDSTONE SAMPLES FROM GENDZLER FIELD,
STEVENS COUNTY, KANSAS

INTRODUCTION

This study reports the results of thin section petrography, scanning electron microscopy, and X-ray diffraction analysis of sandstone and calcarenite samples from the Morrow Formation (Pennsylvanian in age) from unspecified wells within Gendzler Field, Stevens County, Kansas.


The objectives of this study were to:

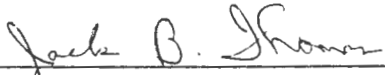
1. Characterize the mineralogy and lithology of the sediment analyzed.
2. Characterize the nature of the authigenic clay in the sandstones, with special regard to the amounts and types of clay present.
3. Determine the factors controlling reservoir quality, including any potential damage which may occur during the drilling and attempted completion of this zone.

Data were acquired through:

1. Thin section petrography of four core samples which were interpreted to be representative of the interval.
2. Scanning electron microscopy (SEM) of two core samples.
3. X-ray diffraction analysis (XRD) of the less than 5 micron (clay) fraction of each of the 20 samples supplied.

Reservoirs, Inc. job number RMD306 has been assigned to this study. Three (3) copies of this report have been delivered to Mr. Nelson Files of Anadarko Production Company, Denver, Colorado. One (1) copy of this report plus all original SEM and thin section data has been retained by Reservoirs, Inc. for future reference. All data generated for this study, interpretations, and other matters relating to RMD306 are considered highly confidential and proprietary to Anadarko Production Company. Discussion of this information with persons other than those of Anadarko Production Company is not permitted without prior approval of the client company.


Lee F. Krystinik
Staff Geologist
RESERVOIRS, INC.


Jack B. Thomas
Vice President-Manager
RESERVOIRS, INC.

RESULTS AND INTERPRETATIONS

Wells: An unknown number of wells within Gendzler Field.

Location: Gendzler Field, Stevens County, Kansas.

Formation and Age: Morrow Formation, Pennsylvanian.

Intervals Studied: No specified interval; Samples 1A-19.

Lithology/Mineralogy:

Each of the samples studied using scanning electron microscopy and thin section petrography are rich in glauconite pellets, biogenic calcite, and quartz. The abundance of these major constituents varies with each sample. The samples plot within the sublitharenite and litharenite fields of Folk's 1968 classification (see Table 1 and Figure 1). The samples are cemented by authigenic quartz overgrowths, iron-rich calcite cement, iron-rich dolomite cement, and several authigenic clays (including chlorite, chlorite/illite, and chlorite/smectite). X-ray diffraction analysis also indicates the presence of kaolinite (interpreted to be present as a detrital clay in the samples, see Table 2).

Glauconite Composition:

Energy dispersive spectrograms were taken for glauconite pellets from Samples 1A and 2. The table below presents the elemental analyses of these grains as elemental percentages, as calculated by an analysis program within the EDAX system. These data indicate a wide variation in composition, probably due to diagenetic alteration (individual measurements of each grain were consistent). It is also possible that the variation in the chemistry of these particles is due to originally different compositions. However, based upon textures observed in thin section and SEM analysis, most of the glauconite particles are interpreted to be primary. It is unlikely that the glauconite was transported in an altered state (many of the particles exhibit such heavy dissolution that it is improbable that they could have survived transport). In addition, the authigenic clays which line much of the porosity in samples studied exhibit the same textures and composition range.

Elemental Analysis of Glauconite From
Samples #1A and #2 (Atomic %)

<u>Sample #1A:</u>	<u>Grain 1</u>		<u>Grain 2</u>	
	Al	8.76%	Al	15.08%
	Si	77.14%	Si	48.32%
	K	1.14%	K	6.55%
	Ca	0.76%	Ca	1.69%
	Fe	12.19%	Fe	28.36%

<u>Sample #2:</u>	<u>Grain 1</u>	<u>Grain 2</u>	
	Al	21.30%	
	Si	46.66%	
	K	4.08%	
	Ca	5.05%	
	Fe	19.64%	
		Mg	3.27%

Depositional Environment:

Thin section analysis of four samples indicates that deposition of these sandstones may have occurred in a shallow marine environment. Glauconite is abundant in all of the samples studied petrographically and shell fragments represent a minor to major percentage of each of the samples studied. Although it is possible that some of this material has been reworked by terrestrial processes, the texture of the glauconite indicates that it is primary.

The glauconite occurs as both pelletal and oolitic glauconite. Both types of glauconite indicate a locally-reducing marine environment. The pelletal glauconite is interpreted to have been generated as fecal material (as evidenced by the presence of regular organic matrix in many of the pellets). The oolitic glauconite is interpreted to have precipitated around seed grains which were being moved back and forth across the sea floor. Glauconite in association with brachiopod fragments, echinoderm fragments, and bryozoan fragments suggests that these sandstones may have been deposited in a relatively shallow, marine setting (within the photic zone).

Porosity Development:

1. Porosity Types (in order of decreasing abundance):
 - a. Intragranular: Generated by the dissolution of soluble grains (feldspar and glauconite fragments). Intragranular porosity is the dominant porosity type in all of the samples studied

petrographically. The effectiveness of this porosity is significantly reduced by the presence of calcite and quartz cements between individual intergranular pores.

- b. Intergranular: Occurring between individual detrital grains. Intergranular porosity is probably the most effective porosity for fluid flow in the samples studied. Although the intergranular porosity is partially occluded by quartz and carbonate cements, it is likely that pore throats are preserved to allow reasonable permeability.
- c. Microporosity: Preserved within the interstices between authigenic clay platlets and within partially dissolved fragments of glauconite and feldspar. Much of the microporosity is so small in diameter that the pore space is probably not capable of transmitting fluid (pore throats often $<0.5\mu$).

2. Factors Controlling Porosity and Permeability:
(in order of decreasing importance)

- a. Intergranular Cements: Authigenic quartz, calcite, dolomite, clay, and pyrite greatly reduce intergranular porosity and in some cases may significantly occlude permeability. Syntaxial authigenic quartz overgrowths greatly reduce the original intergranular porosity in the samples which are not heavily cemented by calcite. In the calcite cemented sample studied (Sample 2) quartz overgrowths are significantly reduced in their importance but porosity is even more heavily occluded by calcite. The clay cement and pyrite occur within the porosity which is left behind after the dissolution of glauconite and feldspar fragments and within some of the original intergranular pore space. The dominant authigenic clays include chlorite, mixed-layer chlorite/illite, illite, and smectite. Chlorite and smectite are sensitive to acidization. Illite can migrate through the formation as fine-grained detritus.
- b. Dissolution: The dissolution of glauconite, feldspar, and biogenic carbonate fragments is an important source of porosity in all the samples studied. Although this type of porosity is common in each of the samples studied, little of this porosity is well-interconnected, such that the permeability of the rock is probably not significantly increased by the presence of much of this secondary porosity.
- c. Lithologic Parameters: Grain size, sorting, compaction, and composition. Large grain size, good sorting, low compaction, and sandstones composed of relatively stable fragments would be expected to have good potential as reservoirs. The sandstones studied in this well are widely variable in their grain size, sorting, and composition. Compaction has been relatively minor in these sandstones. Although "pressure-solution" sutures appear to exist in some of the sandstones, it is interpreted that much of this suturing has occurred as a result of quartz overgrowths growing together within available open pore space.

TABLE 1
Petrography Results (%)

Sample	Framework Grains									Cements				Porosity	
	Grain Size	Sorting	Angularity	Quartz	Feldspar	Glaucinite	Calcite	Det Dolo	Opauques	Dolomite	Calcite	Quartz	Clay	Intragranular	Intergranular
1A	LM	W	SA	67	3	4	2	T	1	2	--	8	2	8	2
2	LVC	P	SR	37	2	1	31	T	T	1	20	1	1	1	4
5	LF	W	SA	58	3	9	2	1	1	2	--	8	2	8	7
7	UC	M	SA	52	5	17	--	9	T	8	--	5	1	2	1

Table 1 shows the petrographic data for samples 1A, 2, 5, and 7. Grain size, sorting, and angularity are stated in the left hand portion of the table in association with the framework-grain composition. Glaucinite and calcite are the two most variable framework-grain constituents. Most of the detrital calcite is present as biogenic detritus, dominantly brachiopod, bryozoan, and echinoderm fragments. The glauconite is present in both pelletal and oolitic forms. Samples 1A, 5, and 7 are relatively similar in the nature of their cementation and porosity. Sample 2 is much higher in its content of calcite cement and biogenic calcite fragments. This sandstone is classified as a calcarenite or, by Folk's classification as a calcareous litharenite. It is significantly higher in its total cement content relative to the other three samples, due to the abundance of calcite which has been altered to calcite cement (see Figure 2).

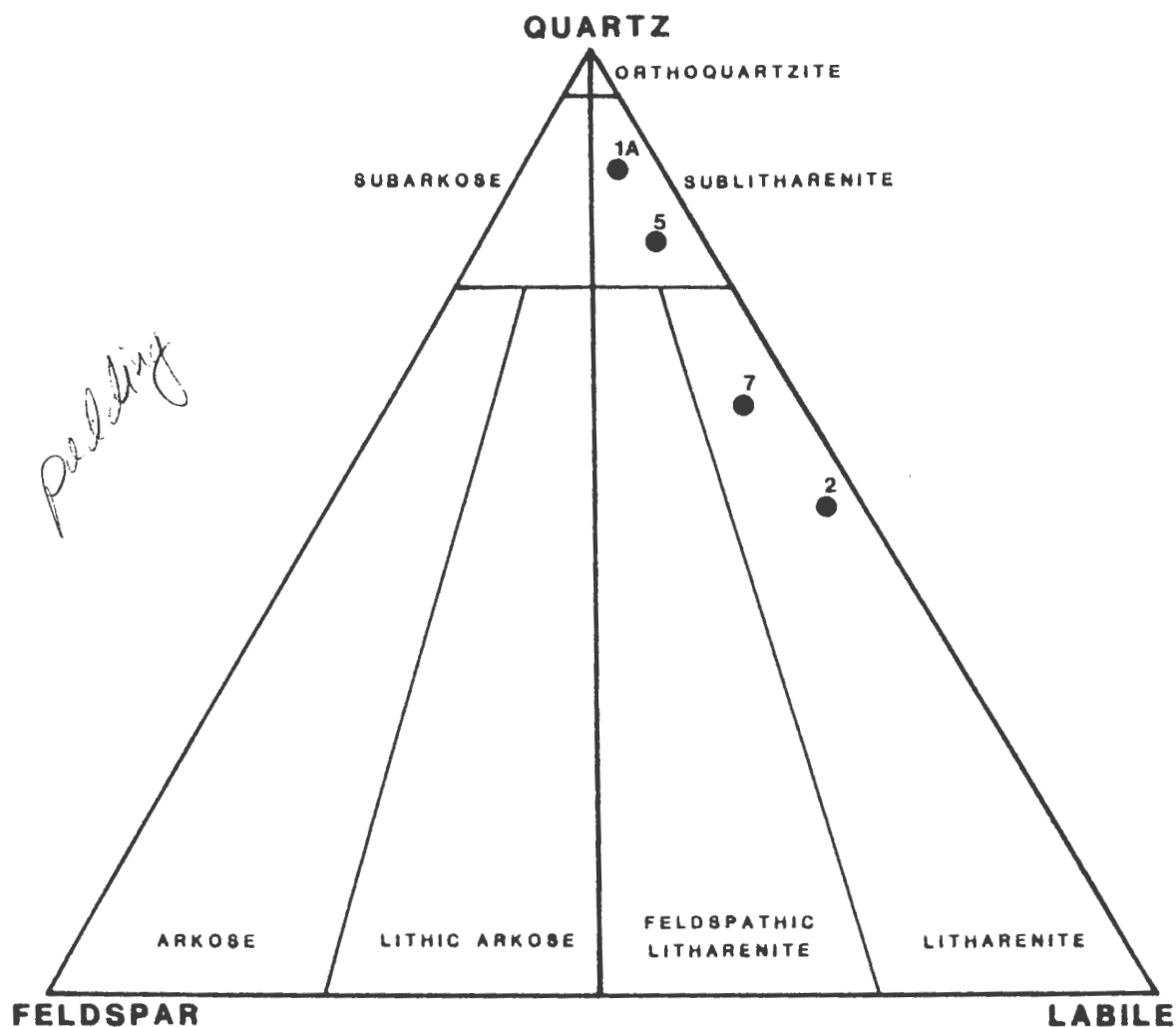


Figure 1: Ternary plot of framework grain compositions (diagram modified from Folk, 1968). The relative content of labile grains (calcite, dolomite, and glauconite) determines the placement of the point; feldspar content is almost constant. Samples 1A and 5 are relatively low in carbonate and contain moderate amounts of glauconite. Samples 2 and 7 are enriched in calcite and glauconite+dolomite respectively.

<u>Sample</u>	<u>Detrital Calcite</u>	<u>Detrital Dolomite</u>	<u>Glauconite</u>
1A	2	T	4
2	31	T	1
5	2	1	9
7	--	9	17

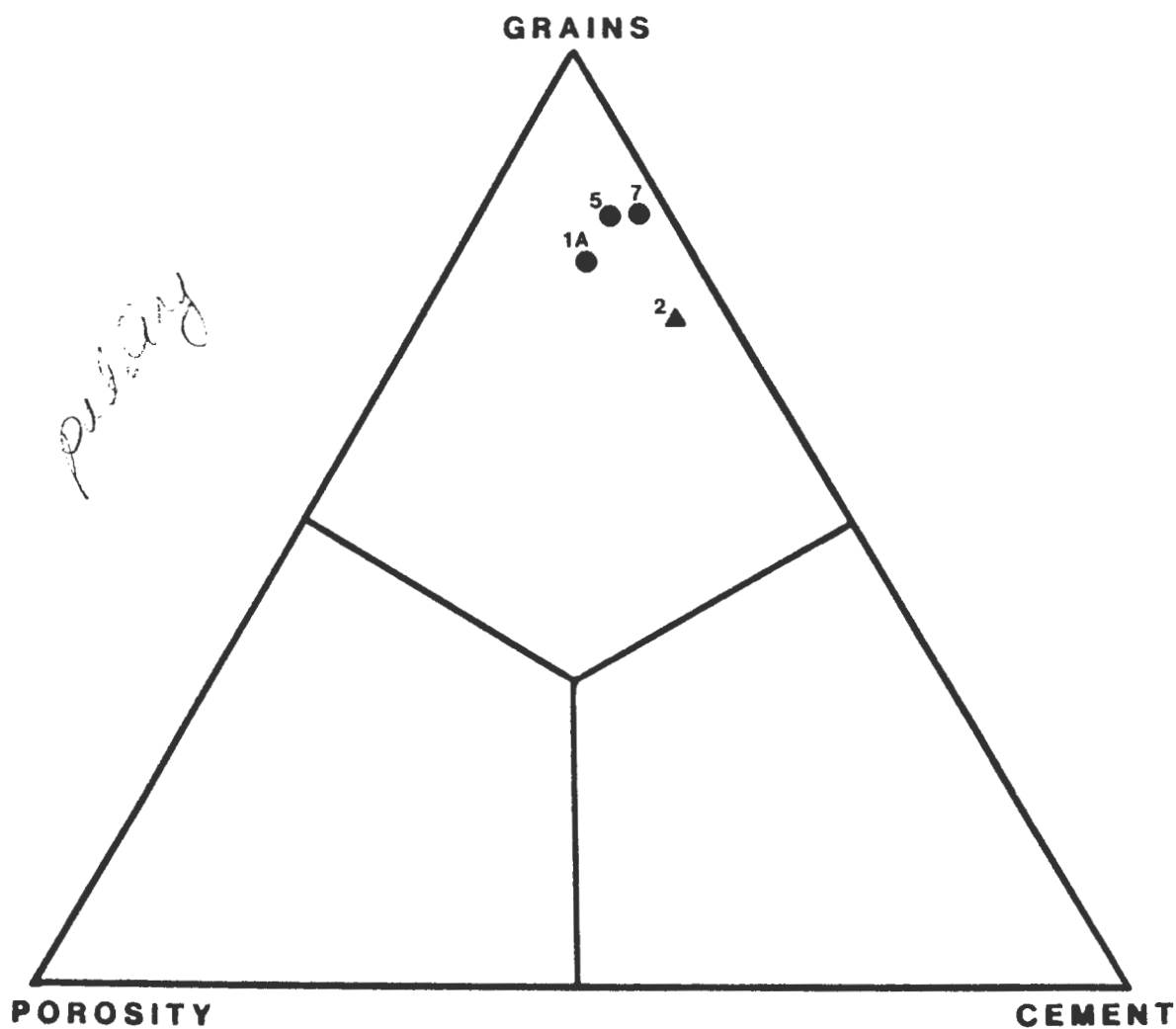


Figure 2: A ternary plot of petrographic data for all components in the sandstones studied. Sample 2 (denoted by a triangle) contains abundant carbonate cement due to the remobilization of calcite from the large percentage of biogenic carbonate present. The table below presents the raw data.

<u>Sample</u>	<u>Grains</u>	<u>Cement</u>	<u>Porosity</u>
1A	78	12	10
2	72	23	5
5	83	12	15
7	80	17	3

TABLE 2

X-ray Diffraction Results for the <5 μ Fraction of Each Sample

Sample	% Clay of the <5 μ Fraction	Kaolinite	Illite	Chlorite	Smectite	Non-Expandable Mixed-Layer (Illite/Chlorite)
1A	9	12	10	74	0	4
1	T	46	26	18	0	10
2	3	44	17	29	4	6
3	12	28	8	64	0	T
4	T	11	29	60	0	0
5	8	T	8	89	0	3
6	9	0	10	88	2	0
7	3	29	47	24	0	T
8	2	13	17	61	0	9
9	3	14	25	53	0	8
10	1	18	18	64	0	0
11	2	10	20	60	10	0
12	12	27	8	65	0	0
13	3	27	11	58	0	4
14	1	20	20	60	0	0
15	2	0	14	81	0	5
16	2	T	28	72	0	0
17	2	29	25	46	0	0
18	2	39	22	39	0	0
19	1	25	25	50	0	0

Table 2 shows the relative abundance of kaolinite, illite chlorite, smectite, and a non-expandable mixed-layer clay (probably chlorite/illite). Glauconite is not stated in this compilation because the mineral glauconite was not detected (probably due to alteration to chlorite) and because many of the green grains called glauconite are actually a mixture of chlorite, smectite, illite, and kaolinite.

Potential Completion Problems:

1. Acid Sensitivity of Iron-Bearing Minerals: The Morrow Formation contains the following iron-bearing minerals: chlorite, iron-rich smectite, iron-rich calcite, iron-rich dolomite, and pyrite. These minerals are all soluble or partially soluble in hydrochloric acid (HCl) and hydrofluoric acid (HF).
 - a. HCl: Dissolution of these minerals in HCl places iron into solution. As the pH of the acid rises during spending, the iron may precipitate as a hydrous iron oxide gel in the presence of free oxygen. These iron-hydroxide precipitates may plug pores and solidify to permanently reduce reservoir quality.
 - b. HF: Dissolution of these minerals in HF can create silicate gels in addition to the iron gels. The potential problem is considered at least as serious as iron gel precipitation.

Upon contact with carbonate minerals, HF may form insoluble calcium fluoride complexes within the porosity network. Equally as important, if sodium and/or potassium are present, insoluble sodium and/or potassium fluorosilicate complexes may be formed within the porosity network.
2. Swelling Clays: The Morrow Sandstone contains minor amounts of smectite in Sample 2 and Sample 11. This clay can swell upon exposure to fresh water or high pH fluids, reducing the deliverability of the pore system.
3. Migration Clays: The presence of thin, fibrous illite within the pore system may result in the migration of "fines" when exposed to turbulent flow or incompatible fluids, such as high pH drilling mud filtrate or cement filtrate. These clays can "bridge" narrow pore throats, reducing permeability.

Precautions for Drilling and Completion:

1. Drill with a low water-loss potassium chloride (KCl) based mud system. The pH of the system should be controlled in the range of 8.5-9.5, if possible, to minimize exposure of sensitive clay minerals to high pH fluids. KCl added to the mud system will tend to reduce permeability damage in the critical, near well bore area, caused by clay-swelling and migration.
2. Cement with a low water-loss cement system to avoid exposing clays to a high pH filtrate.
3. Perforate under nitrogen or under a "clean" fluid (e.g., 4% KCl water plus organic polymer clay stabilizer, surfactant, and 10 pounds per thousand gallons anhydrous citric acid).

"Breakdown" of Perforations:

If it becomes necessary to breakdown perforations by acidizing, a WEAK (3-5%) HCl system is suggested. HF is not recommended, as significant formation damage might result. Any HCl system used should contain an iron sequesterant. Citric or acetic acid is suggested to aid in the prevention of the precipitation of iron gels.

THIN SECTION AND SEM PHOTOMICROGRAPHS WITH DESCRIPTIONS

THIN SECTION AND SEM PHOTOMICROGRAPHS WITH DESCRIPTIONS

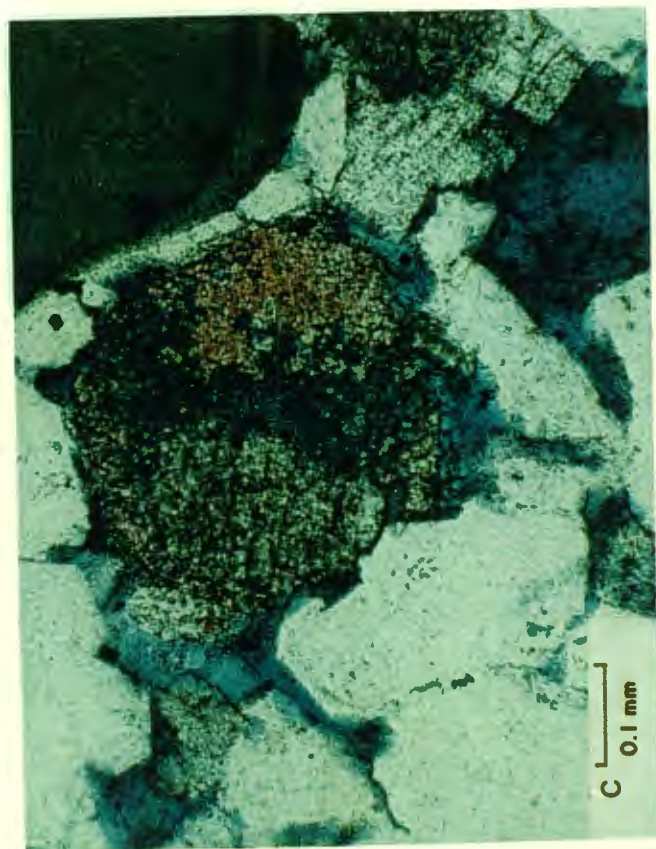
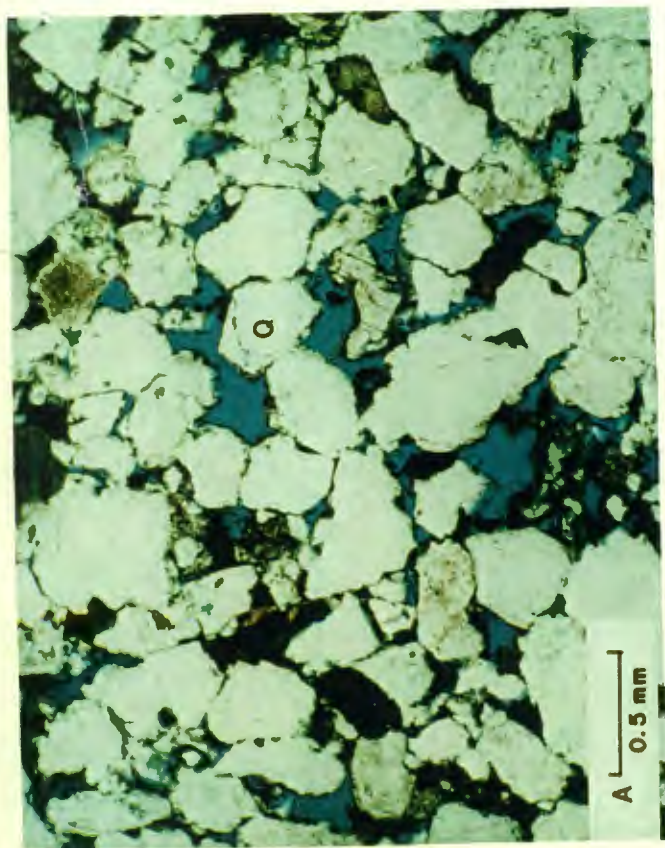
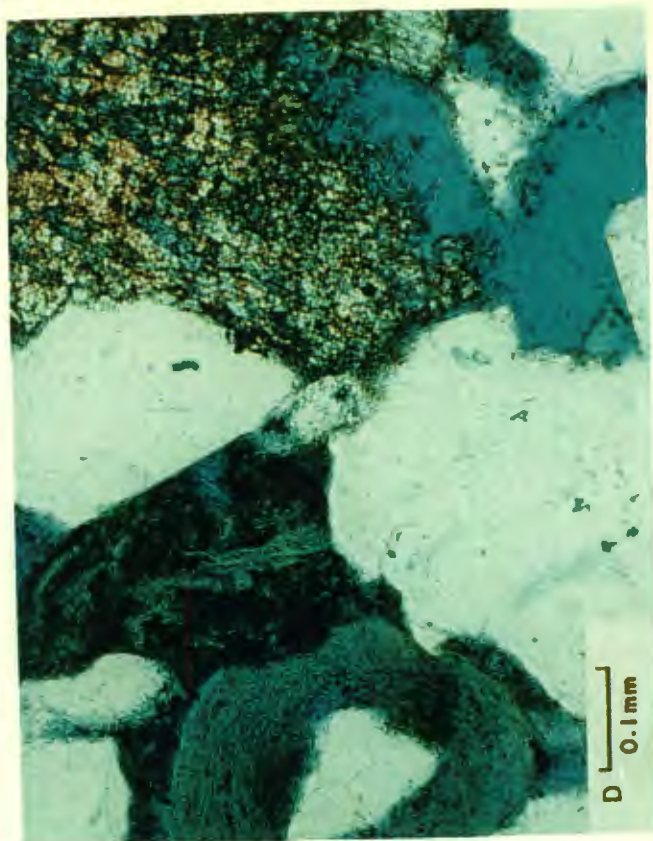
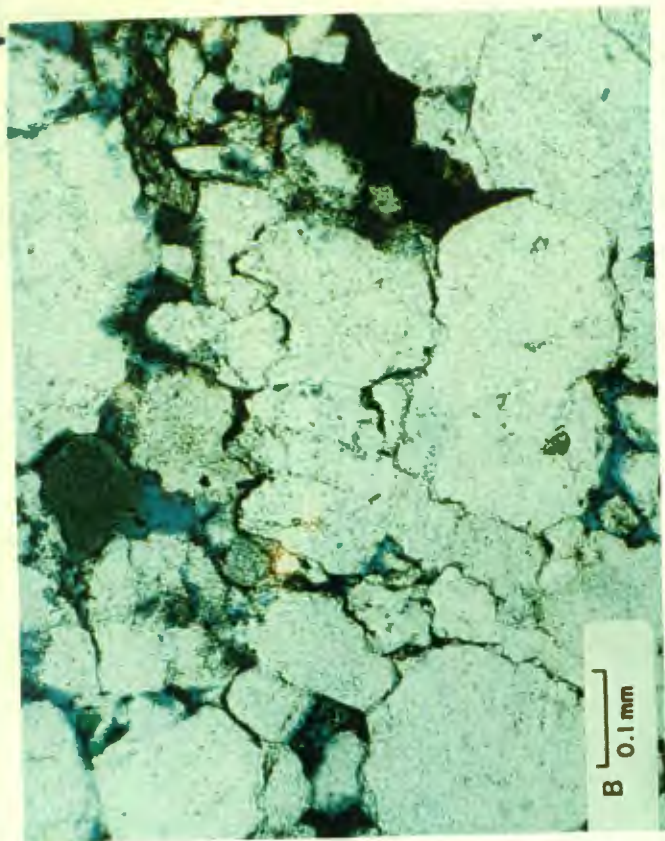
Sample Designation: #1A

View A, 35X, Plane Light. This low magnification view shows the general texture of this lower medium-grained, well-sorted, subangular sublitharenite. The dark green to greenish-black grains in this view are glauconite and glauconite which has been altered to chlorite and mixed-layer clays. Porosity is blue: note the abundance of large pores but narrow pore throats in this sample. The quartz grain the upper right center (Q) exhibits a well formed euhedral quartz overgrowth. Note the angular projection on the upper part of the grain. A faint dust rim demarks the original limit of this quartz grain.

View B, 135X, Plane Light. This close-up shows the presence of glauconite and altered glauconite and significant suturing between quartz grains. This suturing is not interpreted to be due to pressure solution. These sutures are interpreted to have been caused by the growing together of two quartz overgrowths. Few compactional features were observed in this sandstone, indicating that pressure solution is unlikely.

View C, 135X, Plane Light. This close-up shows the presence of a detrital biogenic calcite grain which has been partially dissolved and partially altered to dolomite. The red stain indicates the presence of calcite. The non-stained portion of this grain is dolomite. Also note the glauconite in the upper right, the dolomite cement in the extreme right center, and the euhedral quartz overgrowths in the upper left of this view.

View D, 135X, Plane Light. This close-up shows a partially dissolved echinoderm fragment (upper right), a euhedral quartz overgrowth (lower right), a glauconite ooid with a quartz core (left center), and a glauconite pellet which still has portions of its original organic matrix incorporated within the pellet. Note that the glauconite ooid with the quartz core is partially porous. This is due to incomplete dissolution of the ooid. Many of the glauconite pellets observed in the thin sections from the samples studied exhibit partial to near total dissolution.



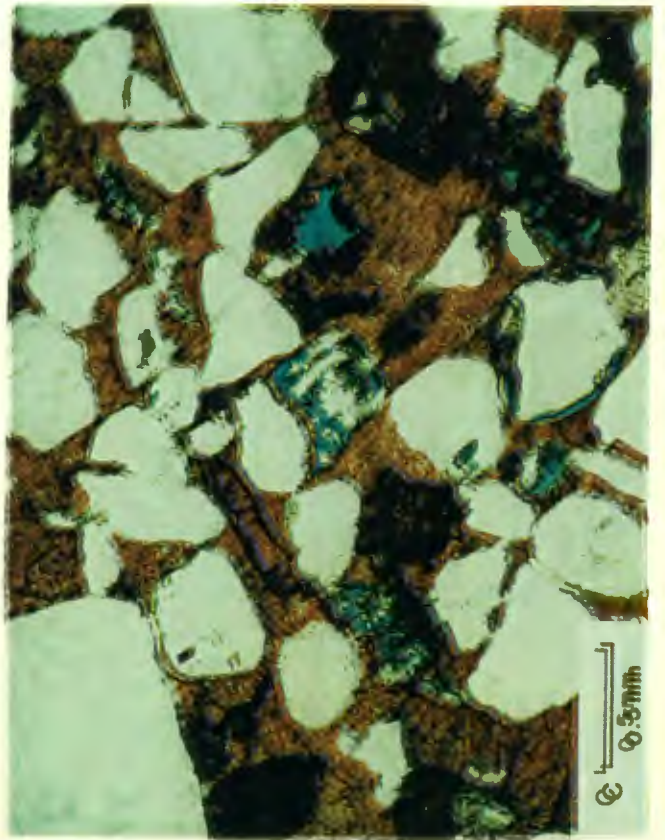
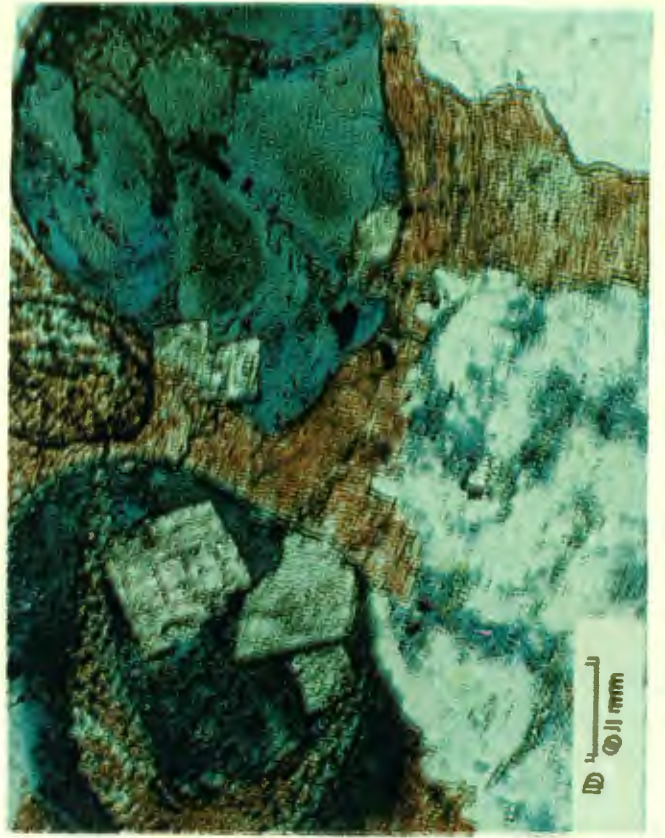
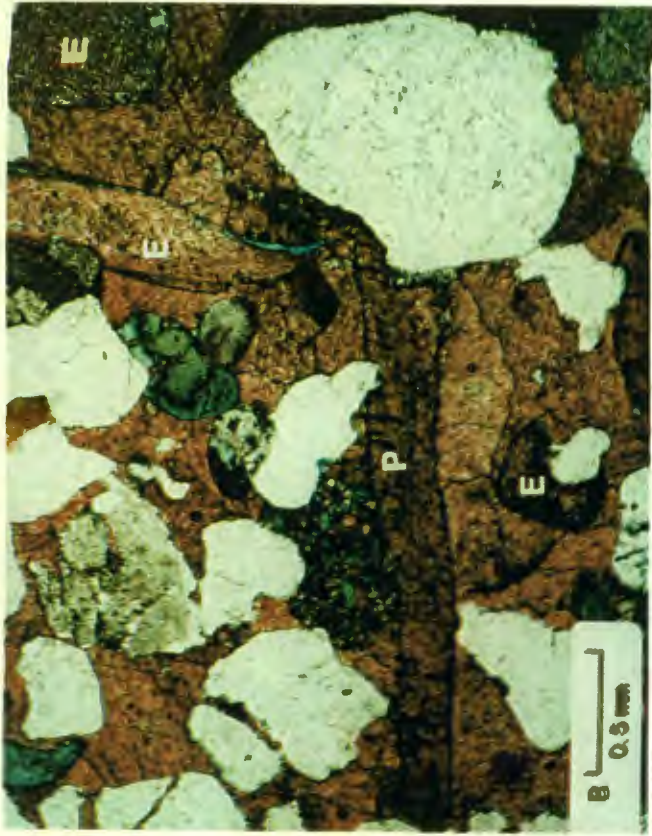
Sample Designation: #2

View A, 35X, Plane Light. This low magnification overview shows the lower very coarse-grained, poorly sorted, and subrounded nature of this calcarenite containing quartz, feldspar, glauconite, and abundant punctate brachiopod fragments, bryozoan fragments, and echinoderm fragments. Interconnected porosity is not well-preserved in this sample, however, secondary porosity generated by the dissolution of feldspar fragments, glauconite fragments, and biogenic calcite is well-developed. Poikilotopic calcite-spar cement and dolomite fill what was originally the intergranular porosity, such that little of the intragranular porosity generated by the dissolution of fragments is interconnected.

View B, 35X, Plane Light. Another low magnification view showing the presence of a punctate brachiopod shell fragment (P) and abundant echinoderm fragments (E). Scattered clasts of glauconite can also be observed. The glauconite clast in the left center of this view is an agglomerate of many small fragments of glauconite which have been bound together by calcite. This clast is interpreted to have been originally a calcareous mud clast with incorporated fragments of glauconite.

View C, 35X, Plane Light. This view shows the presence of secondary porosity which is not interconnected. Much of the secondary porosity in this view was generated by the partial to total dissolution of feldspar grains. The open pore in the right center portion of this view was probably generated by the dissolution glauconite. Glauconite rims the pore.

View D, 135X, Plane Light. This close-up shows the presence of three different types of intragranular porosity. The clast in the upper left of this view is a partially dissolved echinoderm fragment. The clast in the upper right of this view is a partially dissolved glauconite clast. The clast in the lower left of this view is a partially dissolved potassium feldspar grain. Note the presence of euhedral rhombs of iron-rich dolomite which partially fill the secondary porosity in both the echinoderm and the glauconite fragments. The calcite-spar cement which fills the original intergranular space probably prevents effective communication between the secondary pores in this sample.



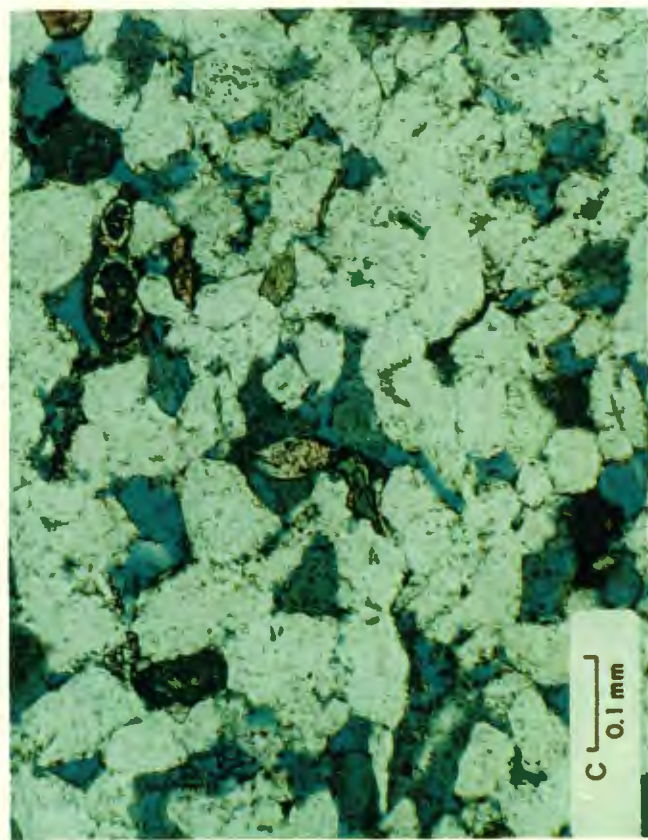
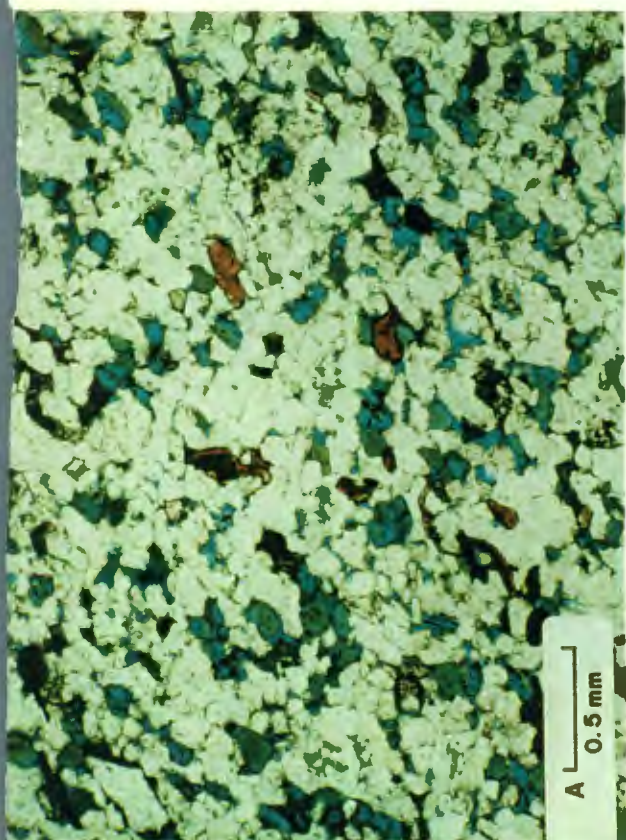
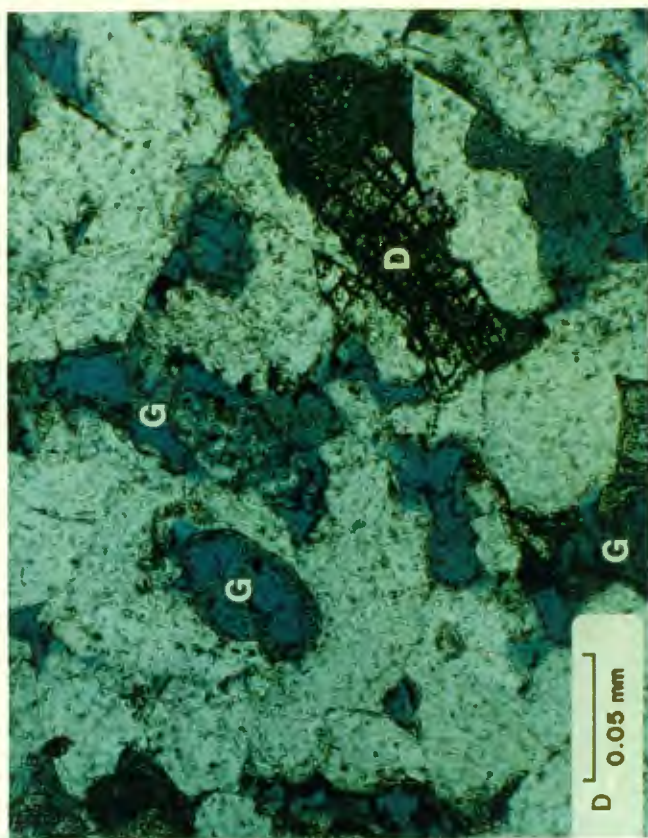
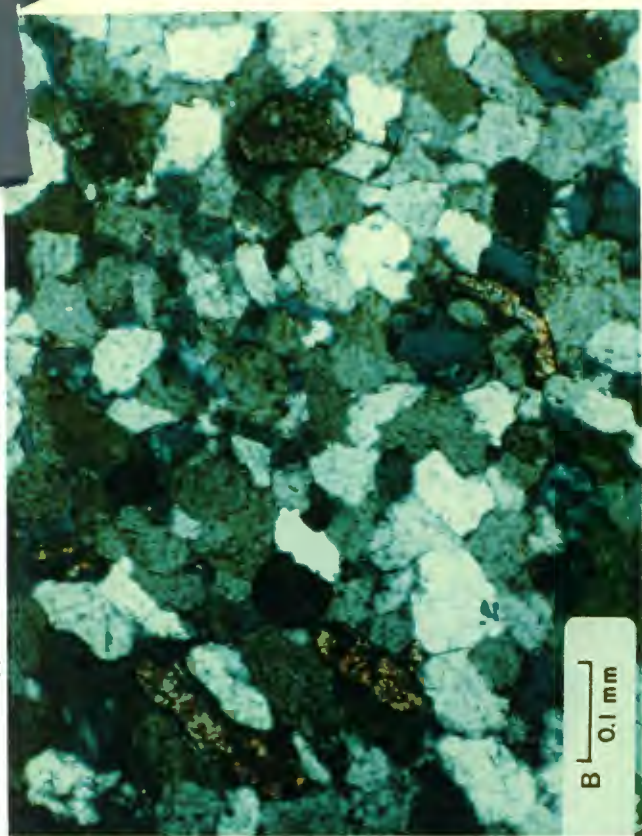
Sample Designation: #5

View A, 35X, Plane Light. An overview of this lower fine-grained, well-sorted, subangular sublitharenite. Note the presence of abundant glauconite and secondary porosity generated by the partial to total dissolution of this glauconite. The red grains are detrital fragments of calcite (mostly echinoderm and brachiopod fragments). Some of the porosity in this sample is relatively well-interconnected compared to the previous samples. Although pore throats are narrow, they do interconnect many of the pores present in this sample.

View B, 135X, Crossed Nicols. This view shows the intergrown nature of many of the quartz grains in the sample. These intergrowths were caused by the gradual intersection of quartz overgrowths as they grew out into the available pore space. The birefringent grains are brachiopod shell fragments.

View C, 135X, Plane Light. This view shows the presence of biogenic calcite and partially dissolved glauconite. Note the presence of pore-lining clays which have been generated as a by-product of the degradation of the glauconite. Also note the angular faces on many of the quartz grains. These were generated by the growth of syntaxial quartz overgrowths on the grains.

View D, 135X, Plane Light. This close-up shows the presence of iron-rich dolomite cement (D), good secondary porosity which is partially interconnected, and partially dissolved pelletal glauconite (G). Note that the porosity is moderately well-interconnected and that the quartz overgrowths have not totally occluded pore throats.



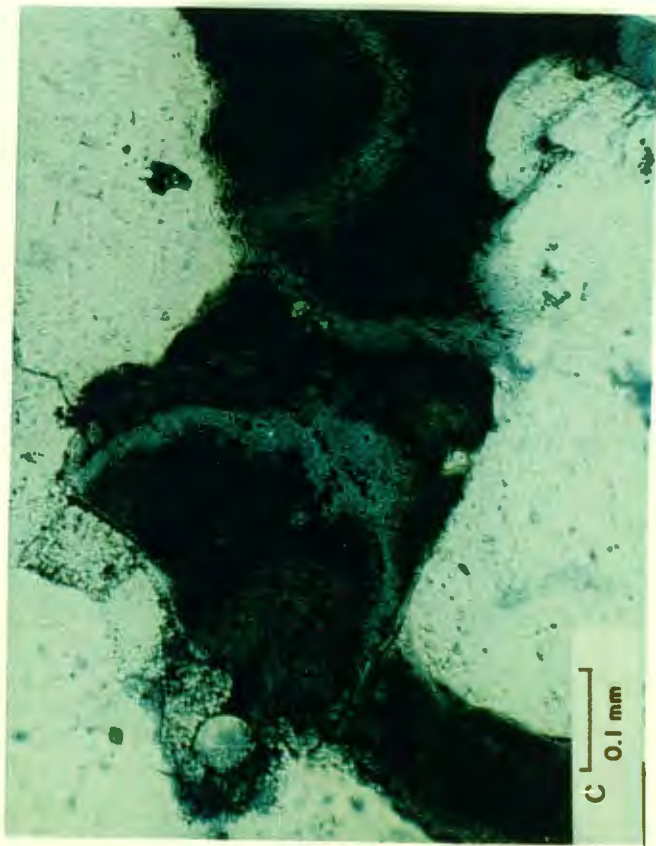
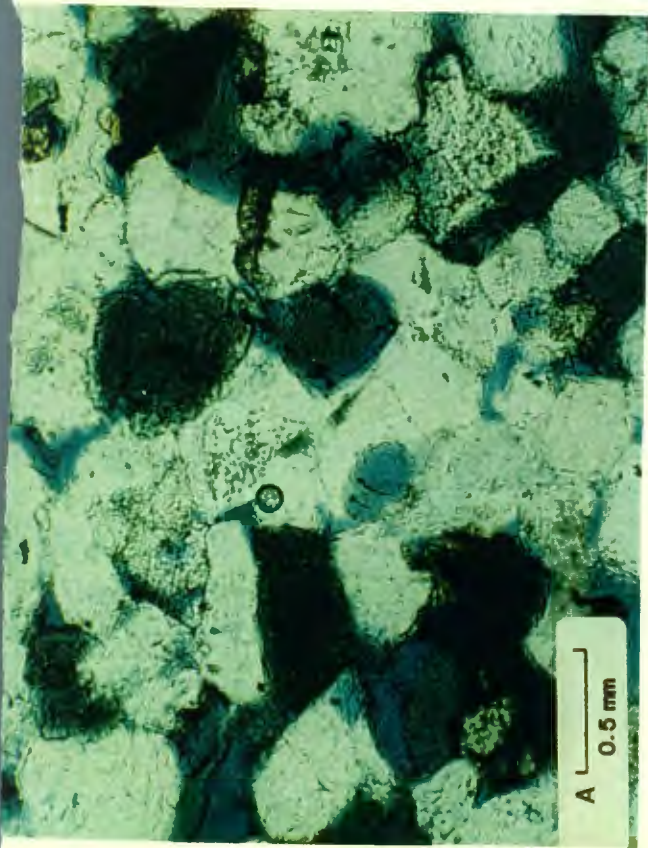
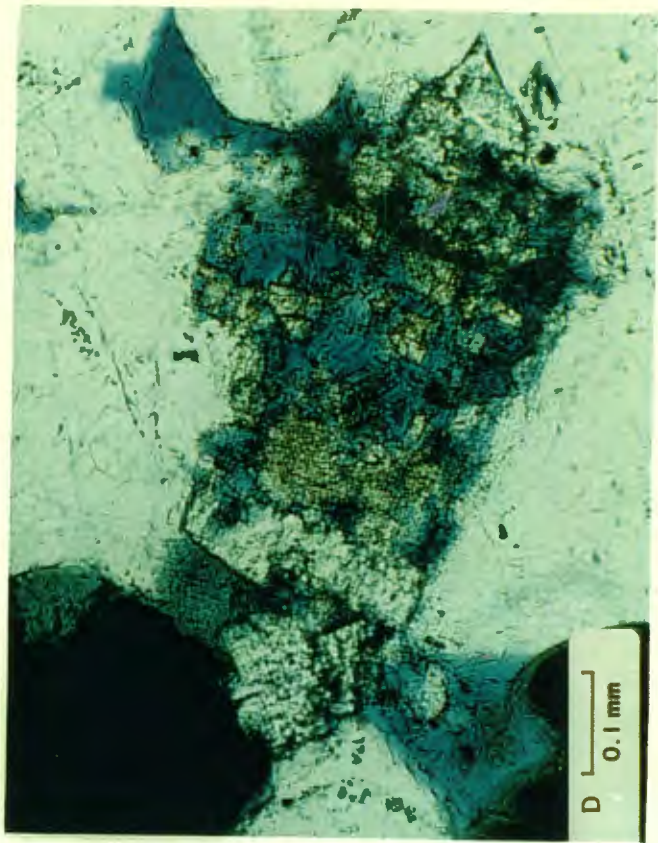
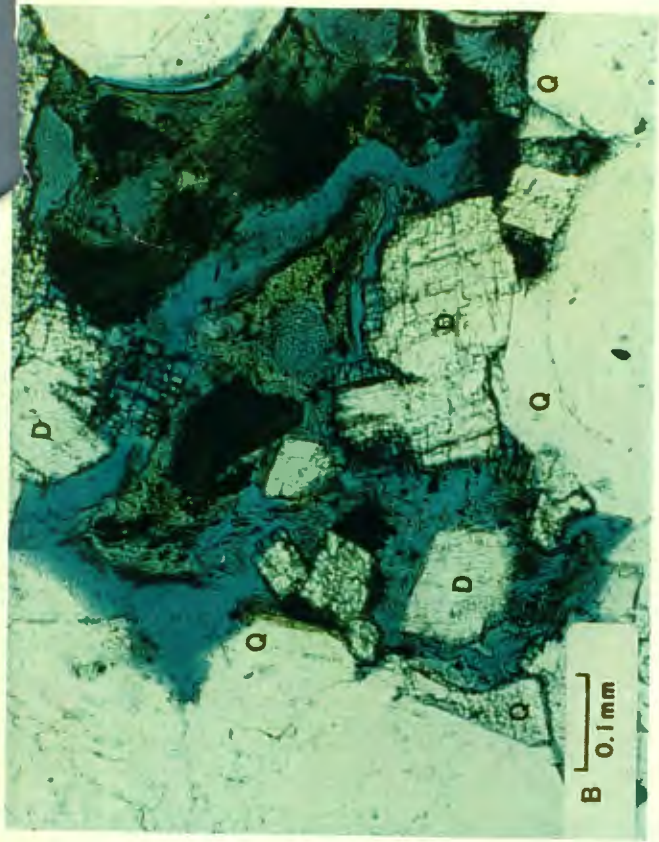
Sample Designation: #7

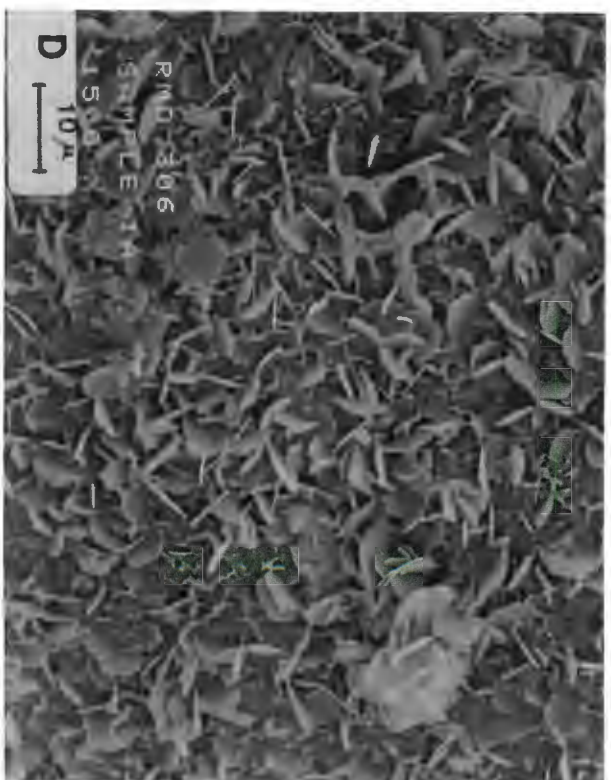
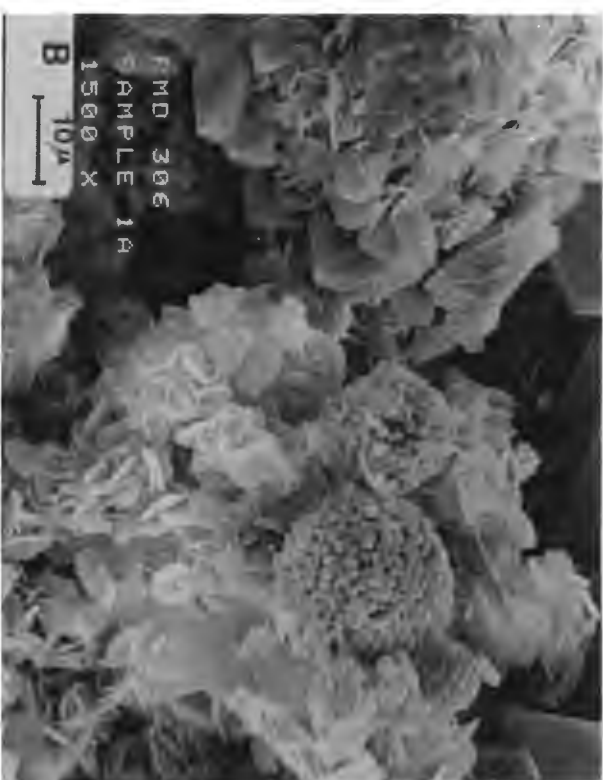
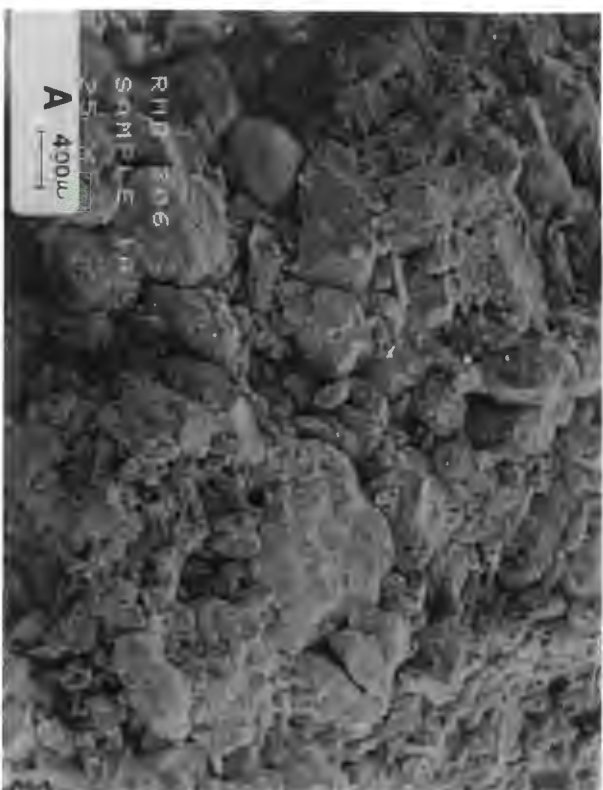
View A, 35X, Plane Light. A low magnification overview of this upper coarse-grained, moderately well-sorted, subangular litharenite. Note the abundance of glauconite and the presence of some secondary porosity generated by the partial dissolution of this glauconite. Some of the original intergranular porosity is also preserved in this sample.

View B, 135X, Plane Light. This close-up shows the presence of dolomite cement which is filling porosity generated by the partial dissolution of a glauconite fragment. Quartz overgrowths (Q) can also be seen partially filling this pore.

View C, 135X, Plane Light. This close-up shows the presence of a partially deformed glauconite grain. Note the presence of the crosshatched organic pattern (probably indicating that the pellet originated as fecal material). The lighter bluish-green portions of the fragment are areas which have been partially dissolved, leaving behind microporosity. Although this porosity may register as porosity with the commonly used porosity logging tools, it is unlikely that this microporosity is effective in the transmission of hydrocarbons.

View D, 135X, Plane Light. This close-up shows the presence of a secondary pore generated by the partial dissolution of a feldspar grain. Iron-rich dolomite is now scattered throughout much of this secondary pore. Also note the presence of a euhedral quartz overgrowth protruding into the pore in the upper right hand portion of this view. Glauconite grains which exhibit partial dissolution can be seen in the left hand portions of this view.





Sample Designation: #2

- A. This overview shows the sample to be relatively heavily cemented by iron-rich calcite and iron-rich dolomite. The grain in the central portion of this view is a partially dissolved glauconite fragment. Many of the euhedral crystals in the central portion of this view are iron-rich dolomite crystals.
- B. A close-up of one of the iron-rich dolomite crystals from the central portion of view A. Also note the presence of the extremely intricate network of authigenic clays surrounding the dolomite crystal. These authigenic clays are dominantly chlorite, smectite, and a mixed-layer chlorite/illite. It is interpreted that these clays are the by-products of the dissolution of the glauconite fragment shown in the central portion of view A.
- C. An overview of a large glauconite clast which has been partially dissolved and has been largely converted to chlorite and mixed-layer chlorite/illite.
- D. A close-up of the texture of the authigenic clays which have formed as a result of the degradation of the glauconite grain in view C. Note the extremely fine-grained nature of this mixed-layer chlorite/illite. Also note the presence of the microporosity within this grain. Although detectable with porosity logs, it is unlikely that this type of microporosity would be effective in the transmission of hydrocarbons. It should also be noted that these types of clays are sensitive to acidization and may produce movable fine-grained detritus and iron hydroxide precipitates upon exposure to acids.

A - 100X

B - 500X

C - 200X

D - 2000X

